RESEARCH ARTICLE

Active Vibration Absorber for a Continuous Structure Model

Carlos Rincón[1], Jorge Alencastre[1](✉), Richard Rivera[1,2]
1 Engineering Department, Pontificia Universidad Católica del Perú, Lima 15088, Perú
2 Acoustics Laboratory, Pontificia Universidad Católica del Perú, Lima 15088, Perú

Abstract The reduction of mechanical vibrations is field of continuous research in engineering in order to reduce damage and improve the performance of structures, machinery, piping and others systems, when they are in presence of dynamical forces. In this sense, different alternatives have been proposed over time, the active vibration absorber highlights as an alternative which can absorb the vibration from a primary system for different excitation frequency in real time. In this study, an active vibration absorber has been modelled as an electromechanical device composed of a 1-DOF model for the absorber and an equivalent electrical circuit for the electromagnetic actuator. It was implemented in a real structure represented by a cantilever beam continuous model, which is the most accurate model that can be used. A set of differential equations which represent the dynamical behaviour of the cantilever beam implemented with the active vibration absorber was obtained from the complete model and it was simulated in Matlab Simulink®. An application of the active vibration absorber for an industry piping system based on the finite element model formulation is presented and developed. Results indicate that the active vibration absorber is able to significantly reduce the vibrations amplitude of the primary system, especially in resonance conditions, for a discrete frequency range. The analytic model and procedure developed here can easily widespread to any more complex primary system.

Keywords vibration absorber, tuned mass damper, active vibration absorber model, active control, electromagnetic vibration absorber

1 Introduction

Mechanical vibrations are manifested in almost any human activity, especially in the engineering field, where they appear in structures, machinery, piping systems and others as a consequence of dynamic forces over time. High vibration amplitudes affect negatively the performance of a system and damage its structure, components and other systems which are connected in some way. This is why they are monitored in specific locations which provide useful information in order to prevent catastrophic failures and correct them in an initial stage [1], [2]. In this sense, the reduction of vibrations amplitude has been a continuous field of research for the engineering, different alternatives for vibration attenuation have been proposed over time, where the dynamic vibration absorber invented by Frahm in 1909 [3], highlights as a mechanical device capable of changing the dynamical characteristics of an existing system. It consists of a mass and stiffness which are tuned to an specific excitation frequency in order to produce an equal force and opposite to the excitation force in the primary system over time [4]. However, it isn't effective if the primary system is excited in a different frequency of the one it is tuned for due to its parameters aren't able to be changed. In this respect, an active component is added to the device in order to tune the vibration absorber to any excitation frequency in real time, this is known as active vibration absorption. Its theory and control strategies have been developed, especially in active control for structural engineering [5], [6]. First active vibration absorber was designed in order to reduce the

[E]-mail: jalenca@pucp.edu.pe
Tel: 6262000 – 4845

vibration amplitudes of a tall building, modelled as discrete masses, caused by wind excitation and earthquakes, which represent a variable excitation frequency over time [7], [8].

Chang & Yang proposed an active mass damper(AMD) for a structure modelled as discrete masses, the actuator dynamics was not considered [9]. Kwak, Yang & Shin proposed a semi active absorber, where the active component was controlled by a correlation with the current magnitude through a solenoid [10], Yu, Thenozhi & Li studied the active vibration absorber implemented to a discrete structure model with PD/PID control of the active force using position over time as feedback [11]. Yang, Shin, Lee, Kim & Kwak used an acceleration feedback, since it is the simplest variable which can be measured directly by accelerometers [12]. Chang developed a LQR control of a AMD with an acceleration feedback for a scaled bridge modelled as a rigid body [13]. Ramesh and Narayanan presented a better accurate structure model of a beam based on the finite element method (FEM) [14]. Cao & Li proposed a new control algorithm, with a better response than LQR under same conditions, based on the calculation of the optimal gains in order to obtain the minimum variance of the displacement response over time [15]. Zhou & Li applied an active tuned mass damper (AMTD) with a LQR control algorithm to a tall building represented as FEM model calibrated by its dynamical response measurement [16]. In these studies, primary systems were modelled as discrete systems; however, real systems are more complex than a discrete model as well as their dynamical behaviour. Also different control strategies and feedback variables have been implemented, where PD/PID control algorithms highlight as the standard industrial controllers due to its simplicity and well known theory [11].

In this paper, an active vibration absorber is modelled as an electromechanical device and applied over a continuous structure model, which is the most accurate model of a real structure. A PD control algorithm is used for the active force. A cantilever beam continuous model is chosen because it can be used to represent different structures and the procedure here can be applied to different systems.

2. Active Vibration Absorber Modelling

The active vibration absorber can be modelled as a secondary 1-DOF system, Fig. 1, it consists of a mass m_a, a damper that is represented by the damping coefficient b_a, the stiffness k_a and an external active force produced by an electromagnetic lineal actuator u. The magnitude and direction of the active force is calculated in order to tune the system to any excitation frequency.

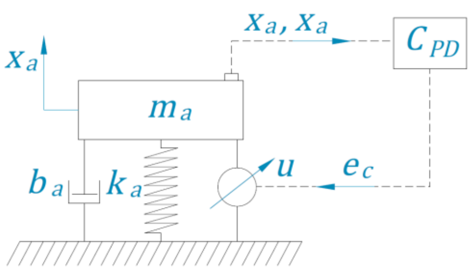

Fig. 1 Active vibration absorber

Using 2nd Newton's Law, the equation of motion for this vibration absorber is given by (1).

$$m_a \ddot{x}_a + b_a \dot{x}_a + k_a x_a = u \text{ , (1)}$$

The dynamic behaviour of an electromagnetic actuator is obtained from its geometric and electromagnetic characteristics according to the modelling presented in [17], [18]. It can be simplified as an equivalent electrical LR circuit given by (2), where L is the inductance, R is the resistance, I is the current and e_c is the excitation voltage. $K_b \dot{x}_a$ is the voltage induced by the relative movement in presence of current through a solenoid [19], where K_b is the actuator constant.

$$L\dot{i} + Ri + K_b \dot{x}_a = e_c \text{ , (2)}$$

The interaction between an electromagnetic field and the current through a circuit of the electromagnetic actuator produces the active force over time according to the Lorentz' Law, (3), where u is the active force and K_c is an actuator constant.

$$u = K_c i \text{ , (3)}$$

According to the vibration absorption theory, the natural frequency of the decoupled system must be equal to the excitation frequency of the primary system. The same working concept is used to tune the active vibration absorber. In this sense, a PD control is able to modify the real part as well as the imaginary part of the poles of its characteristic equation in order to locate these poles in the imaginary axis with a frequency equal to the excitation frequency. The PD control of the electromagnetic actuator voltage was proposed in [19] and it has the following form (4), where K_p and K_d are the PD gains for the position and velocity feedback.

$$e_c = K_p x_a + K_d \dot{x}_a \text{ , (4)}$$

Using Laplace transform in the equations (1), (2), (3), and ordering, equations (5) and (6) in Laplace domain are obtained.

$$X_a(s) = \frac{K_c}{\left(m_a s^2 + b_a s + k_a\right)\left(sL + R\right) + K_b K_c s} E(s) \text{ , (5)}$$

$$E_c(s) = K_p X_a(s) + sK_d X_a(s) \text{ , (6)}$$

Solving the characteristic equation of the system, the PD gains which tune the natural frequency of the active vibration absorber to the excitation frequency ω_c are given by (7) and (8).

$$K_p = \mathrm{Re}\left(\frac{-\left(Ls + R\right)\left(m_a s^2 + c_a s + k_a\right) - K_b K_c s}{K_c}\right)_{s=\omega_c i} \text{ , (7)}$$

$$K_d = \frac{1}{\omega_c} \mathrm{Im}\left(\frac{-\left(Ls + R\right)\left(m_a s^2 + c_a s + k_a\right) - K_b K_c s}{K_c}\right)_{s=\omega_c i} \text{ , (8)}$$

The equations above in Laplace domain of the active vibration absorber response are represented as a control diagram with the position and velocity of the absorber feedback, Fig. 2.

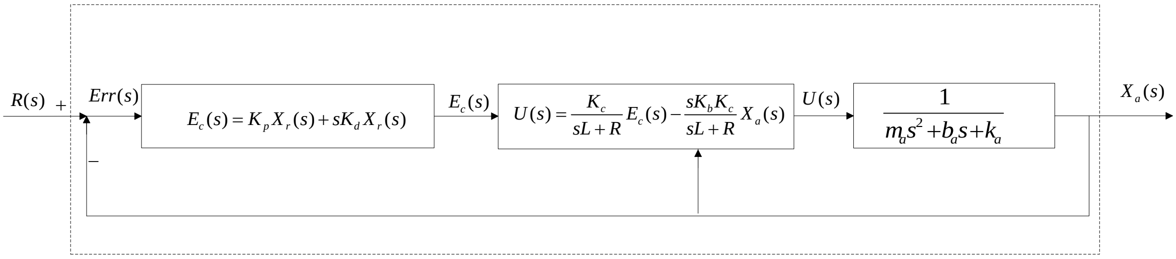

Fig. 2 Scheme of active vibration absorber control diagram

3. Active Control of a Cantilever Beam

The active vibration absorber is implemented to a cantilever beam, Fig. 3. The force produced by the absorber to the beam is considered as a punctual force. A continuous model is used for the analysis. Kinetic and potential energy expressions of the cantilever beam have the following form (9) and (10), where $\rho(x)$ is the density, $A(x)$ is the section transversal area, w is the deflection, $E(x)$ is the Young modulus and $I(x)$ is the inertia of the transversal area along the x axis

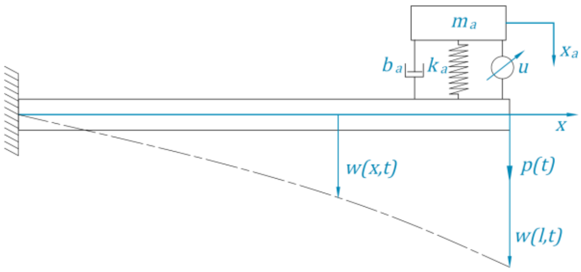

Fig. 3 Cantilever beam implemented with an active vibration absorber at its free end

$$T = \frac{1}{2}\int_0^l \rho(x)A(x)\left(\frac{\partial w}{\partial t}\right)^2 dx\,, \quad (9)$$

$$V = \frac{1}{2}\int_0^l E(x)I(x)\left(\frac{\partial^2 w}{\partial^2 x}\right)^2 dx\,, \quad (10)$$

The deflection of any position along the beam can be represented as the superposition of the modal coordinates [20], which is given by (11), where $q_i(t)$ is the generalized coordinate related to i-mode of vibration and $\varphi_i(x)$ is the normal mode function.

$$w(x,t) = \sum_{i=1}^{n} q_i(t)\varphi_i(x)\,, \quad (11)$$

where

$$\varphi_i(x) = C_i\left[sen\beta_i x - senh\beta_i x - \alpha_i(\cos\beta_i x - \cosh\beta_i x)\right], \quad i = 1\ 2\ 3\ \ldots n\,, \quad (12)$$

$$\alpha_i = \frac{sen\beta_i l - senh\beta_i l}{\cos\beta_i l - \cosh\beta_i l}\,, \quad (13)$$

According to the procedure developed in [21], using the Lagrange equations for (9) and (10), the dynamics of the cantilever beam is represented by the differential equations system in (14), where m_{ij}

is the generalized mass, k_{ij} is the generalized stiffness, $h^1{}_j$ is the generalized force of disturbance and $h^2{}_j$ is the generalized force of the force produced by the active vibration absorber at its position along the beam.

$$\sum_{i=1}^{n} m_{ij}\ddot{q}_i(t) + \sum_{i=1}^{n} k_{ij} q_i(t) = h^1{}_j + h^2{}_j, \qquad j = 1 \;\; 2 \ldots n, \text{ (14)}$$

$$\begin{cases} m_{ij} = \int_0^l \rho(x)A(x)\varphi_i(x)\varphi_j(x)dx = 0 \\ k_{ij} = \int_0^l E(x)I(x)\dfrac{d^2\varphi_i}{dx^2}\dfrac{d^2\varphi_j}{dx^2}dx = 0 \end{cases} \quad Si \;\; i \neq j \;\; , \text{ (15)}$$

$$\begin{cases} h^1{}_j = p(t)\varphi(l)_j \\ h^2{}_j = f(t)\varphi(l)_j \end{cases} \; j = 1 \;\; 2, \text{ (16)}$$

Solving the differential equations system in (14) in Laplace domain and substituting it in (11), the deflection, in Laplace domain, along the beam as a function of the disturbance $P(s)$ and active force $U(s)$ is obtained, (17).

$$W(l,s) = \sum_{i=1}^{2} G^i{}_p P(s) + \sum_{i=1}^{2} G^i{}_u U(s), \text{ (17)}$$

where

$$\begin{cases} G^i{}_p(s) = G_i^{-1}\varphi_i^2(l) \\ G^i{}_u(s) = G_i^{-1}\left(-\dfrac{m_a s^2}{m_a s^2 + b_a s + k_a}\right)\varphi^2{}_i(l) \end{cases}, \text{ (18)}$$

$$G_i = m_{ii}s^2 + k_{ii} + \frac{m_a s^2(k_a + b_a s)}{m_a s^2 + b_a s + k_a}\varphi_i(l)^2 \;\; , \text{ (19)}$$

Hence the active control is obtained coupling the equations of the PD control, the electromagnetic actuator and the cantilever beam. Fig. 4 shows a scheme of the developed active control of the cantilever beam using the relative position and velocity feedback.

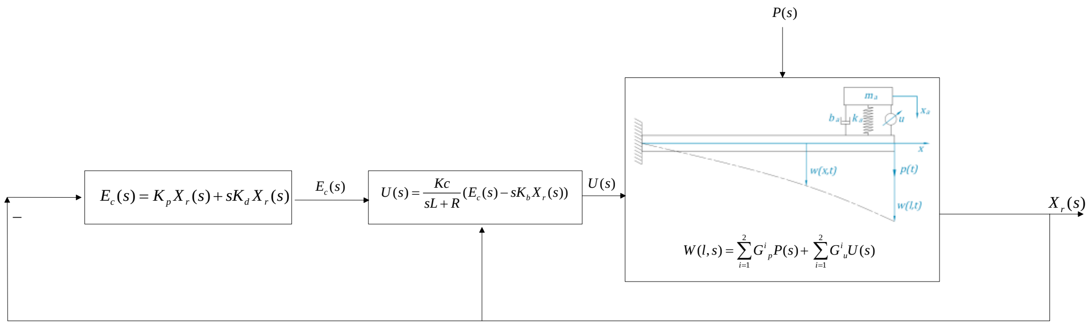

Fig. 4 Active control diagram of a cantilever beam implemented with the active vibration absorber

4. Numerical Results and Discussion

The developed model was simulated using Matlab Simulink®. Parameters used for the simulation are listed in Table 1, the parameters of the electromagnetic actuator presented in [19] were used. The cantilever beam was excited in its first and second resonant frequency in order to evaluate the vibration amplitude with and without absorber, the natural frequencies with the established parameters were calculated and are shown in Table 2. When the active vibration absorber is added, the natural frequencies change because of its mass and stiffness, those are tuned to the first natural frequency. Hence there are a new pair of natural frequencies 3.50 and 4.93 Hz around 4.14 Hz, which is the absorption frequency if the absorber works as passive.

Table 1 Parameters of the cantilever beam and active absorber

Cantilever beam		Active vibration absorber	
Parameter	Value	Parameter	Value
b	50 mm	m_a	0.05 kg
e	5 mm	k_a	141.8 N/m
ρ	7850 kg/m3	b_a	0.1 N.s/m
A	600 mm2	R	1.6 Ohm
E	210 GPa	L	0.75 mH
I	5000 mm4	K_c	3.5 N/A
l	1 m	K_b	3.5 V.s/m

Table 2 Natural frequencies of the cantilever beam

Natural frequency	Original	With absorber
First	4.14 Hz	3.50 Hz
Second	26.26 Hz	4.93 Hz
Third	73.53 Hz	26.26 Hz

4.1. Dynamic characteristics and tunning of the active vibration absorber

As explained above, PD control gains have to change the dynamic characteristics of the active vibration absorber. Its natural frequency has to be equal to the excitation frequency of the primary system in order to induce an inertial force with the same magnitude and opposite direction to the excitation force. Using equations (7) and (8), the PD gains were calculated for the second resonant frequency, K_p is 606.87 V/m and K_d is -3.22 V-s/m. In order to analysis the dynamic behaviour of the decoupled active absorber, the step response of the only absorber, represented as the relation Xa(s)/Ec(s), and with control, represented as Xa(s)/Err(s), were evaluated, see Figure 2. Figure5a shows the response of the active vibration absorber without control, while Figure 5b shows the response with the implemented PD control tuned to the second resonant frequency. In Figure5a, the input signal was a unit voltage step, there're no overshoots over time and the settling time was 0.87s. In Figure 5b, the input signal was a unit error step which is the difference between the reference and the output, the settling time was 0.875s.

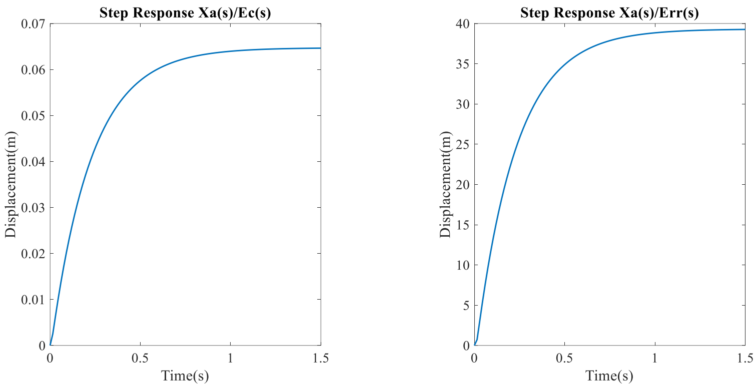

(a) (b)

Fig. 5 (a) Step response of the active vibration absorber without PD control in open loop; (b) Step response of the active vibration absorber with PD control from an error signal

Fig. 6 show the dynamic response of the decoupled active vibration absorber in frequency domain when it is tuned to these resonant frequencies. The peak and phase change in 4.14 Hz and 26.26 Hz which correspond to its first and second natural frequency respectively and also, they match with the desired absorption frequency of the primary system.

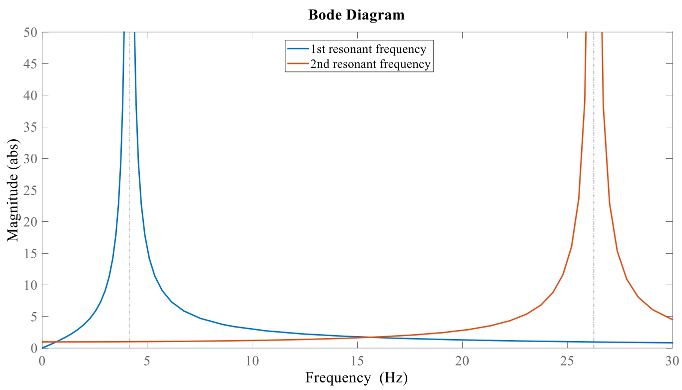

Fig. 6 Frequency response of the active vibration absorber

4.2. Dynamic response of the structure in resonance conditions

The objective of the active vibration absorber is to reduce the vibration amplitude of a primary system, in this case, a cantilever beam when is excited in its resonant frequencies. Fig. 7 shows its dynamic response with a passive absorber, the developed active absorber and without absorber when it is excited in its first resonant frequency at the free end position. Without absorber, the vibration amplitude increases over time due to the resonance condition. However, with a passive absorber and the active absorber, the amplitude maintains its value, hence they are effective and absorbing the vibration. Note that there's no a significant difference between passive and active absorber in this case. This is due to the working concept of the developed active absorber, where the controlled active force is designed to induce a proportional opposite force to the relative displacement between the absorber and the cantilever beam as an "artificial stiffness". In this sense, since mass and stiffness of the absorber are tuned to the first resonant frequency, the active absorber is already tuned without the active force.

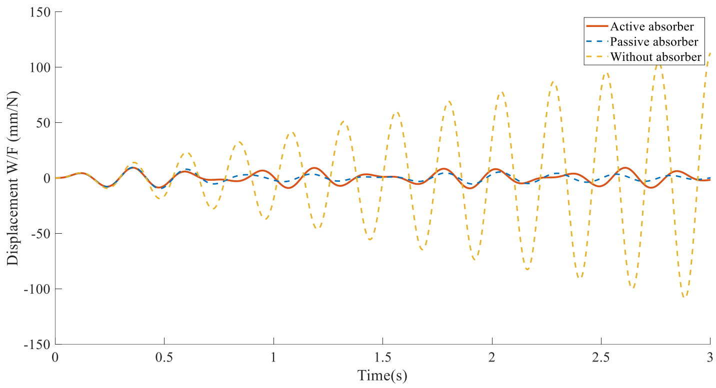

Fig. 7 Dynamic response under the first resonant frequency

Fig. 8 shows the dynamic response when it is excited in its second resonant frequency. As expected, without absorber, the vibration amplitude increases over time. The passive absorber is not effective in this case due to its parameters were designed just for the first resonant frequency. Nevertheless, the active vibration absorber is effective and maintains a low vibration amplitude over time.

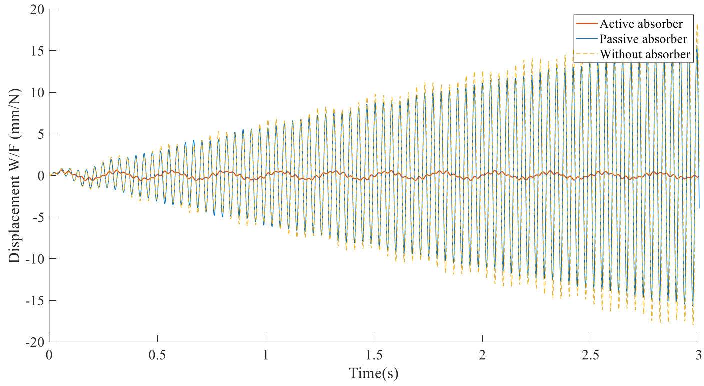

Fig. 8 Dynamic response under the second resonant frequency

It was explained that the working concept of an active vibration absorber consists of inducing an inertial force over time. Fig. 9 shows the active force and relative displacement over time when the cantilever beam is excited in its second resonant frequency at the free end position. It must be noted that the active force is always opposite and proportional to the relative displacement as an artificial stiffness tuned to that frequency.

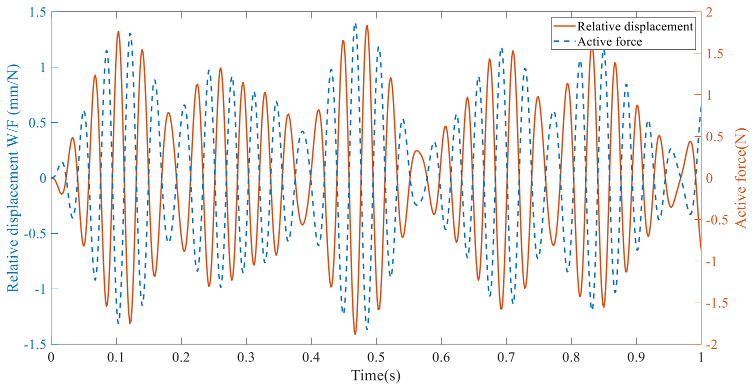

Fig. 9 Active force and relative displacement under the second resonant frequency

4.3. Influence of the active vibration absorber position in the dynamic response

Results above were obtained with the absorber placed in the cantilever free end; however, there's no a unique place available along the cantilever. In order to evaluate the influence of the position, the absorber was placed in three different positions at 1/3, 2/3 of its length relative to the fixed end and at free end, for each absorber position, the free end displacement was obtained over time when the primary system was excited in the second resonant frequency, Fig. 10. For any position, the vibration absorber is effective and reduce the vibration amplitude. Nevertheless, the maximum reduction is obtained when the absorber is placed at free end, where the external dynamical force acts. Fig. 11 shows the dynamic response when the absorber was placed in a node of the primary system and the response without absorber, the second mode of vibration contains a node at 0.783 of its length where the amplitude is zero. In this case, the absorber is not effective and the vibration amplitude increases over time, note that there's no a significant difference between with the absorber and without absorber.

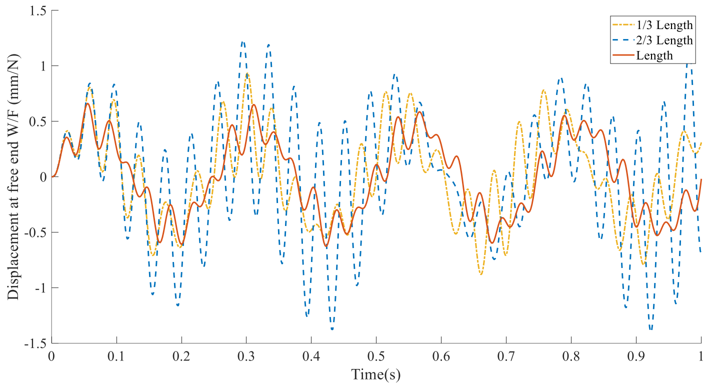

Fig. 10 Displacement at free end under the second resonant frequency for the active vibration absorber placed in 1/3, 2/3 of the length and at free end

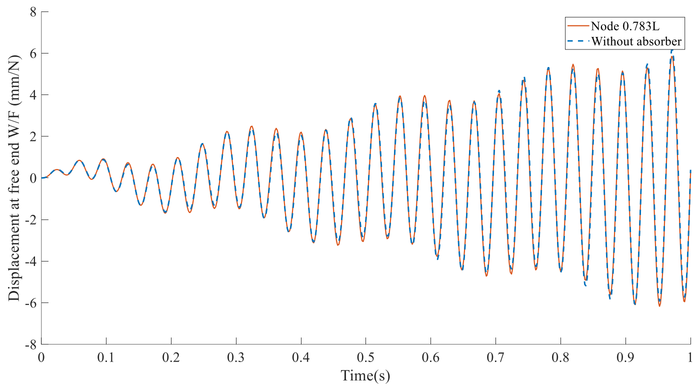

Fig. 11 Displacement at free end under the second resonant frequency for the active vibration absorber placed in a node of the second vibration mode at 0.783 of its length

4.1. Case study: Application for an industry piping system

Once the model equations of the active vibration absorber (AVA) for the analysis in real structures are proven in Matlab® Simulink, the developed AVA can be applied in any system represented either a continuous model or a finite element model. In order to show application procedure, the AVA equations are applied to a piping system under dynamic forces which produce vibrations. **Fig. 12a** represents a common industry problem related to transfer process. When flow is pumped through a piping system, dynamic forces are produced by the machinery or by the flow (known as flow-induced vibration) which can excite one of the vibrations modes of the piping system. The pipes are usually connected by flanges and supported along their lengths, flanges are needed to facilitate the fabrication in situ; however, these connections are susceptible to vibrations that can make them loose the screws.

The finite element model of this piping system is shown in **Fig. 12b**, it consists of 7 Euler-Bernoulli beam elements placed along the length. The dynamic force acts at the 1st position due to the pump-pipe interaction and excites the system in its first mode of vibration. Results above indicate that the AVA is more effective when it is placed in the position with a higher vibration amplitude, but here it is placed between the two supports at the 3st position where there's the availability.

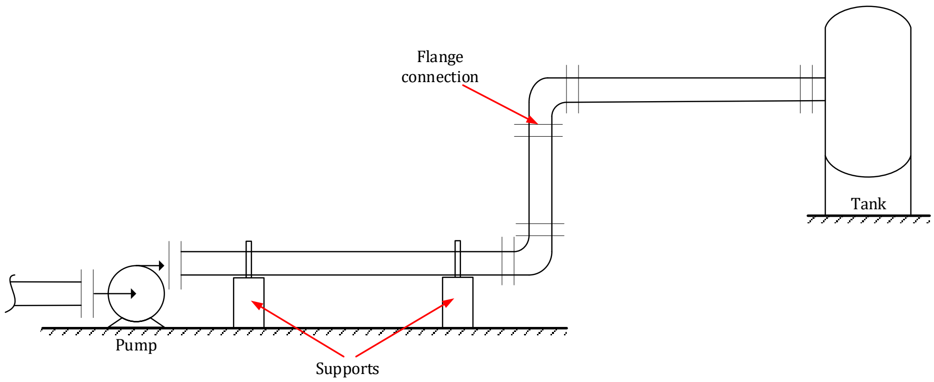

(a)

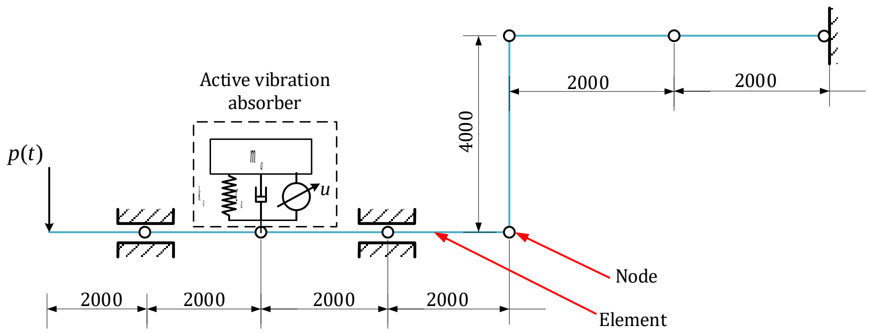

(b)

Fig. 12 (a) Scheme of piping system for analysis (b) Finite Element Model of the system: beam elements arrangement

4.1.1 Finite element model formulation

Here it is briefly described the finite equation formulation for a beam with two nodes. The total potential energy $\boldsymbol{\pi}$ for flexural vibration of a beam element is shown in equation (20), where $\boldsymbol{w}$ is the deflection, $\boldsymbol{u}$ is the lineal density, $\boldsymbol{q}$ is a distributed load, $\boldsymbol{F_i}$ is the nodal force, $\boldsymbol{M_j}$is the nodal moment and $\boldsymbol{\theta}$ is the nodal rotation.

$$\pi_{total} = \frac{EI}{2}\int_0^L \left(\frac{\partial^2}{\partial x^2} w(x,t)\right)^2 dx + \int_0^L \mu(x)\ddot{w}(x,t)w(x,t)dx - \int_0^L q(x,t)w(x,t)dx \\ -\sum_{i=1}^{n} F_i(t)w_i(x,t) - \sum_{j=1}^{n} M_j(t)\theta_i(x,t) \quad , (20)$$

Applying the principle of virtual work to the total potential energy to equation (20), it must be equal to zero, equation (21).

$$\delta\pi_{total} = EI\int_0^L w''(x,t)\delta w''(x,t)dx + \int_0^L \mu(x)\ddot{w}(x,t)\delta w(x,t)dx - \int_0^L q(x,t)\delta w(x,t)dx \\ -\sum_{i=1}^{n} F_i(t)\delta w_i(x,t) - \sum_{j=1}^{n} M_j(t)\delta\theta_i(x,t) = 0 \quad , (21)$$

For a beam element, the deflection $\boldsymbol{w}$ is written as a function of the hermitic functions matrix $[\boldsymbol{N}]$ and the displacement matrix $[\boldsymbol{U}]$, equation (22).

$$w(\xi,t)=\left[N\right]^{T}\left[U\right], (22)$$
$$w^{"}(\xi,t)=\left[B\right]\left[U\right]$$

where

$$\left[N\right]=\left[N_1 \quad \frac{L}{2}\bar{N}_1 \quad N_2 \quad \frac{L}{2}\bar{N}_2\right]$$
$$\left[U\right]=\begin{Bmatrix} w_1(t) \\ \theta_1(t) \\ w_2(t) \\ \theta_2(t) \end{Bmatrix}$$

Replacing equation (22) in (21)

$$\left[\delta U\right]\left(\left(\int_{-1}^{+1}\left[B\right]EI\left[B\right]^{T}\frac{L}{2}d\xi\right)\left[U\right]+\left(\int_{-1}^{+1}\mu(x)\left[N\right]\left[N\right]^{T}\frac{L}{2}d\xi\right)\left[\ddot{U}\right]-\begin{Bmatrix} F_1 \\ M_1 \\ F_2 \\ M_2 \end{Bmatrix}\right)=0$$

Since the variational can't be zero, the equations in parentheses can be written as a differential equations system of a beam element, equation (23).

$$\left[M^{(1)}\right]\ddot{U}^{(1)}+\left[K^{(1)}\right]U^{(1)}=\left[F^{(1)}\right], (23)$$

where

$$\left[K^{(1)}\right]=\int_{-1}^{+1}\left[B\right]EI\left[B\right]^{T}\frac{L}{2}d\xi$$
$$\left[M^{(1)}\right]=\int_{-1}^{+1}\mu\left[N\right]\left[N\right]^{T}\frac{L}{2}d\xi$$
$$\left[F^{(1)}\right]=\begin{Bmatrix} F_1 \\ M_1 \\ F_2 \\ M_2 \end{Bmatrix}$$

Integrating all the equations for each element, a system of differential equations is obtained, equation (24), where $\boldsymbol{M}$ is the system mass matrix, $\boldsymbol{K}$ is the system stiffness matrix, $\boldsymbol{U}$ is the system matrix of nodes coordinates displacement and rotation, $\boldsymbol{F}$ is the external forces matrix.

$$M\ddot{U}+KU=F\ , (24)$$

The AVA is placed at the 3st position, where the 5th coordinate of deflection is. Hence, the inertial force produced by the AVA is applied to the 5th coordinate, equation (25).

$$F_5(s)=-m_a s^2 X_a(s)\,, (25)$$

Fig. 13 shows a scheme of the active vibration control applied to the developed finite element model of the piping structure. The developed AVA equations are represented by the transfer functions and applied to the finite element model in a state space representation. The PD control uses the relative displacement between the AVA and the 3rd position of the system model, which is the 5th nodal coordinate obtained from the state space representation when a dynamic force $\boldsymbol{p(t)}$ acts.

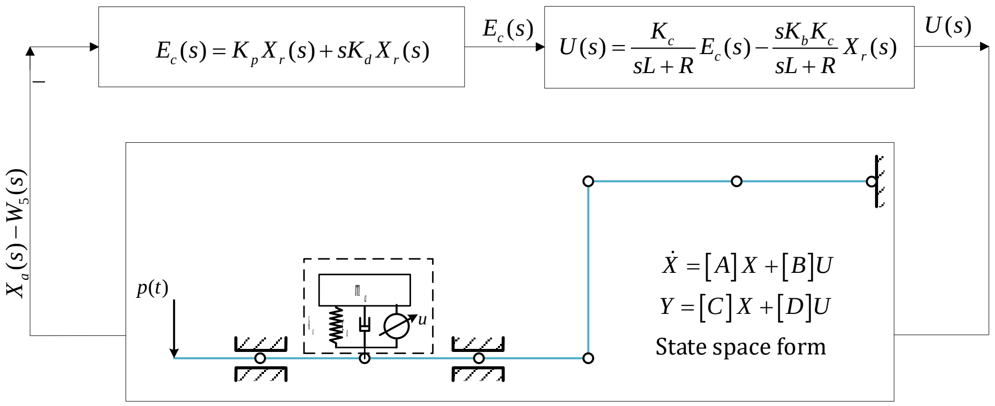

Fig. 13 Scheme of the active vibration control of a piping system

4.1.2 Numerical results

The piping system model obtained by the finite element method (FEM) and the AVA equations are implemented to Matlab® Simulink as the Fig. 13 shows. The parameters of piping system model and the AVA for the simulation are shown in Table 3.

Table 3 Parameters for the simulation

Finite element model of the piping system		Active vibration absorber	
Parameter	Value	Parameter	Value
μ	7.18 kg/m	m_a	0.14 kg
L_{beam}	2000 mm	k_a	1435.3 N/m
ρ	7850 kg/m3	b_a	0.1 N.s/m
A	914.20 mm2	R	1.6 Ohm
E	210 GPa	L	0.75 mH
I	4908700 mm4	K_c	3.5 N/A
		K_b	3.5 V.s/m

The piping system is excited at the 1st position with a frequency near the first resonant frequency. The parameters of the absorber $\boldsymbol{m_a}$ and $\boldsymbol{k_a}$ are not tuned to the first natural frequency, hence the control gains are calculated in order to tune the AVA to that frequency 23.9 Hz. **Fig. 14** shows the 3st position displacement over time of the piping system model obtained by FEM for two cases: with and without active absorber. When there's no an active absorber, the piping system is in a resonant condition, thus the displacement increse over time and the stress and strain in flange connections along the pipes also increse, which is a risk situation. However, when the AVA is applied, the displacement keeps within a range which is safer for the flow transfer process.

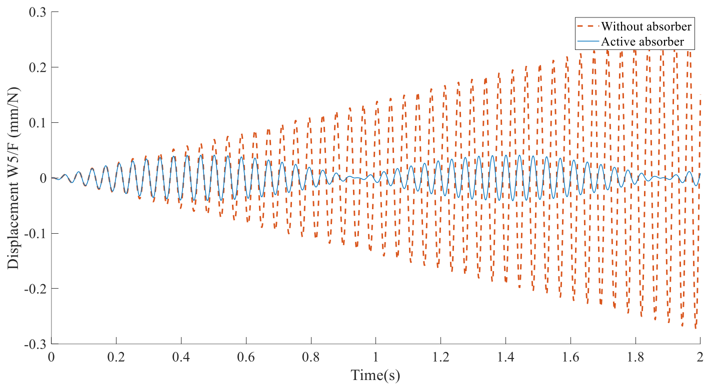

Fig. 14 Dynamic response of the 3rd position of the piping system model under the first resonant frequency

5. Conclusions

A model of an active vibration absorber implemented to a continuous cantilever beam was developed, this continuous model represents the most accurate dynamic response of the real structure. Results indicate that the active vibration absorber is able to be tuned to a desired frequency within an excitation frequency range from a primary system and reduce the vibration amplitude, especially in critical conditions corresponding to the resonant frequencies.

The vibration amplitude is absorbed in the whole continuous cantilever beam model, not only at the position of the active vibration absorber. The position of the active absorber at the cantilever beam has a significant influence at the reduction of vibration, especially if it is placed near to a vibration node from the primary system, where the active absorber is not effective. It was found that the optimum position for the active vibration absorber corresponds to the position of the maximum vibration amplitude at the primary system. In this sense, a proper formulation of the primary system model and experimental validation are required, especially for complex systems, in order to establish the absorption frequency range, optimum position and active absorber physical characteristics. The analysis of the developed active vibration absorber model is not limited to continuous structures, but also it is effective for applying it to any system represented by discrete models or finite element models following the procedure presented.

Acknowledgements The authors would like to thank Enrique Carrillo for the specific guidelines in control theory and assisting the algorithms programming in Matlab® for the solution.

References

1. Orhan S, Aktürk N, Çelik V (2006) Vibration monitoring for defect diagnosis of rolling element bearings as a predictive maintenance tool: Comprehensive case studies. NDT E Int 39:293–298. https://doi.org/10.1016/j.ndteint.2005.08.008
2. Sofronas A (2012) Case Histories in Vibration Analysis and Metal Fatigue for the Practicing Engineer. Wiley, pp 245–268
3. Frahm H (1911) A Device for Damping Vibrations of Bodies
4. Den Hartog JP (1956) Mechanical Vibrations, 4th ed. McGraw-Hill, New York
5. Soong TT (1988) Active structural control in civil engineering. Eng Struct 10:74–84. https://doi.org/10.1016/0141-0296(88)90033-8
6. Housner GW, Bergman LA, Caughey TK, et al (1997) Structural control: Past, present, and future. J Eng Mech 123:897–971. https://doi.org/10.1061/(ASCE)0733-9399(1997)123:9(897)
7. Kobori T, Koshika N, Yamada K, Ikeda Y (1991) Seismic-response-controlled structure with

active mass driver system. Part 1: Design. Earthq Eng Struct Dyn 20:133–149. https://doi.org/10.1002/eqe.4290200204

8. Kobori T, Koshika N, Yamada K, Ikeda Y (1991) Seismic-response-controlled structure with active mass driver system. Part 2: Verification. Earthq Eng Struct Dyn 20:133–149

9. Chang C., Yang HTY (1995) Control of Buildings Using Active Tuned Mass Dampers. 121:355–366

10. Kwak MK, Yang DH, Shin JH (2015) Active vibration control of structures using a semi-active dynamic absorber. Noise Control Eng J 63:287–299. https://doi.org/10.3397/1/376326

11. Yu W, Thenozhi S, Li X (2014) Stable active vibration control system for building structures using PD/PID control. IFAC

12. Yang DH, Shin JH, Lee HW, et al (2017) Active vibration control of structure by Active Mass Damper and Multi-Modal Negative Acceleration Feedback control algorithm. J Sound Vib 392:18–30. https://doi.org/10.1016/j.jsv.2016.12.036

13. Chang S (2020) Active mass damper for reducing wind and earthquake vibrations of a long-period bridge. Actuators 9:. https://doi.org/10.3390/ACT9030066

14. Ramesh Kumar K, Narayanan S (2008) Active vibration control of beams with optimal placement of piezoelectric sensor/actuator pairs. Smart Mater Struct 17:. https://doi.org/10.1088/0964-1726/17/5/055008

15. Cao H, Li QS (2004) New control strategies for active tuned mass damper systems. Comput Struct 82:2341–2350. https://doi.org/10.1016/j.compstruc.2004.05.010

16. Zhou K, Li Q-S, Li X (2020) Dynamic Behavior of Supertall Building with Active Control System during Super Typhoon Mangkhut. J Struct Eng 146:04020077. https://doi.org/10.1061/(asce)st.1943-541x.0002626

17. Palomera-Arias R, Connor JJ, Ochsendorf JA (2008) Feasibility Study of Passive Electromagnetic Damping Systems. J Struct Eng 134:109–158. https://doi.org/https://doi.org/10.1061/(ASCE)0733-9445(2008)134:1(164)

18. Diez-Jimenez E, Rizzo R, Gómez-García MJ, Corral-Abad E (2019) Review of Passive Electromagnetic Devices for Vibration Damping and Isolation. Shock Vib 2019:. https://doi.org/10.1155/2019/1250707

19. Elmali H, Renzulli M, Olgac N (2000) Experimental comparison of delayed resonator and PD controlled vibration absorbers using electromagnetic actuators. J Dyn Syst Meas Control Trans ASME 122:514–520. https://doi.org/10.1115/1.1286820

20. Rao SS (1952) Mechanical Vibrations, 5th ed. Pearson

21. Łatas W (2016) Application of the continuous dynamic absorbers in local and global vibration reduction problems in beams. Vib Phys Syst 27:245–254